Low temperature properties of the triangular-lattice antiferromagnet: A bosonic spinon theory

A Mezio[1], L O Manuel[1], R R P Singh[2] and A E Trumper[1]

[1] Instituto de Física Rosario (CONICET) and Universidad Nacional de Rosario, Boulevard 27 de Febrero 210 bis (2000) Rosario, Argentina

[2] Department of Physics, University of California, Davis, California 95616, USA

E-mail: trumper@ifir-conicet.gov.ar

Abstract. We study the low temperature properties of the triangular-lattice Heisenberg antiferromagnet with a mean field Schwinger spin-$\frac{1}{2}$ boson scheme that reproduces quantitatively the zero temperature energy spectrum derived previously using series expansions. By analyzing the spin-spin and the boson density-density dynamical structure factors, we identify the unphysical spin excitations that come from the relaxation of the local constraint on bosons. This allows us to reconstruct a free energy based on the physical excitations only, whose predictions for entropy and uniform susceptibility seem to be reliable within the temperature range $0 \leq T \lesssim 0.3J$, which is difficult to access by other methods. The high values of entropy, also found in high temperature expansions studies, can be attributed to the roton-like narrowed dispersion at finite temperatures.

PACS numbers: 75.10.Jm

Submitted to: *New J. Phys.*

1. Introduction

The study of triangular-lattice spin-$\frac{1}{2}$ Heisenberg model (THM) has been a central problem in quantum many body physics ever since Anderson made the proposal that its ground state properties could be described by a Resonant Valence Bond picture [1, 2]. The development of several numerical techniques [3, 4, 5, 6, 7, 8, 9, 10, 11] was crucial to elucidate that the zero point quantum fluctuations, in this particular system, are not enough to destroy the classical 120° Néel order, lending support to a simple semiclassical description at low temperatures, such as that provided by linear spin wave theory (LSWT) [12].

Nonetheless, early high temperature expansion (HTE) studies [6] performed down to low temperatures showed no evidence of a renormalized classical behaviour as predicted by the non linear sigma model (NLσM) [13, 14]. For instance, around $T = 0.25J$, the correlation length calculated by HTE is only $\xi \sim 1.5$ lattice constants, in contrast to the value $\xi \sim 12$ predicted by NLσM [6, 10]. Consistent with these values, the entropy calculated by HTE was one order of magnitude larger than that of the NLσM. These early results were interpreted as a probable crossover between renormalized classical and quantum critical regimes [15].

Unexpectedly, series expansion (SE) studies [10, 16] performed at zero temperature also showed a strong downward renormalization of the high energy part of the spectrum with respect to LSWT, along with the appearance of roton-like minima at the midpoints of the edges of the hexagonal Brillouin zone (BZ). Originally, the presence of such roton-like excitations were proposed to be related to possible fermionic spinon excitations which in turn would lead to the anomalous low temperature properties of the THM [10]. However, subsequent works showed that non trivial $1/S$ corrections, arising from the non collinearity of the 120° Néel order, accurately recovers the $T = 0$ series expansion results [17, 18, 19]. This gave support to an interacting magnon picture for the spectrum, although it was found that the magnon-quasiparticles are not well defined for a significant part of the Brillouin zone [18, 19]. Nevertheless, by assuming a bosonic character for the SE dispersion relation, the high values of entropy found at low temperature was attributed to the thermal excitation of rotons, even at temperatures below the roton gap [10].

Here we explore the low temperature properties of THM from an alternative viewpoint: A bosonic spinon perspective, based on the Schwinger boson formalism [20, 21]. One advantage of this point of view is that it preserves the rotational invariance of the THM at finite temperatures, in agreement with the Mermin-Wagner theorem [22]; while at zero temperature it recovers the 120° Néel ordered state as a condensation of the Schwinger bosons [23, 24]. In fact, it has been shown in the literature [25, 26] that the Schwinger boson theory describes very well the ground state properties of the THM, finding good agreement with exact diagonalization [27] and other available numerical techniques (For a complete survey of the available results on the THM see table III of [10]). More recently, we have shown [28] that the main features of the magnetic

excitation spectrum found using series expansions can be reproduced correctly using a proper mean field scheme of decoupling. In addition, by computing the density-density and spin-spin dynamical structure factors we were able to identify unphysical magnetic excitations that can be traced back to the relaxation of the local constraint of the Schwinger bosons at the mean field level [28].

In practice, the relaxation of the local constraint seems to be not crucial for the correct description of certain ground state static properties [28]. But as soon as temperature increases, the system starts to explore in increasingly large amounts an unphysical phase space, leading to an incorrect estimation of the thermodynamic quantities. Instead of introducing *ad hoc* factors to compensate for the above problem [20, 21], we use our ability to distinguish between the physical and the spurious excitations to properly extend the Schwinger boson mean field (SBMF) to finite temperatures by considering only the physical low energy excitations. We rename the latter the reconstructed Schwinger boson mean field (RSBMF). The values of entropy and uniform susceptibility thus calculated interpolate quite well within the temperature range $0-0.3J$, on opposite ends of which LSWT plus $1/S$ corrections and HTE become reliable, respectively. Our results support the idea of [10] that the high values of entropy found with HTE are due to the excitation of rotons which, within the context of our theory, can be identified with collinear short range AF fluctuations above the underlying 120° Néel correlations.

2. Rotational invariant Schwinger boson mean field theory

In using Schwinger boson representation for the spin operators [20, 21],

$$\hat{S}_i^x = \frac{1}{2}(\hat{b}_{i\uparrow}^\dagger \hat{b}_{i\downarrow} + \hat{b}_{i\downarrow}^\dagger \hat{b}_{i\uparrow}),\ \hat{S}_i^y = \frac{1}{2\mathrm{i}}(\hat{b}_{i\uparrow}^\dagger \hat{b}_{i\downarrow} - \hat{b}_{i\downarrow}^\dagger \hat{b}_{i\uparrow}),\ \hat{S}_i^z = \frac{1}{2}(\hat{b}_{i\uparrow}^\dagger \hat{b}_{i\uparrow} - \hat{b}_{i\downarrow}^\dagger \hat{b}_{i\downarrow}), \quad (1)$$

the local constraint on the boson number $\sum_\sigma \hat{b}_{i\sigma}^\dagger \hat{b}_{i\sigma} = 2S$ must be imposed to fulfil the spin-S algebra. The spin-spin interaction of the triangular-lattice Heisenberg model can then be written in terms of singlet bond operators [28, 29] as

$$\hat{\mathbf{S}}_i \cdot \hat{\mathbf{S}}_j = :\hat{B}_{ij}^\dagger \hat{B}_{ij}: - \hat{A}_{ij}^\dagger \hat{A}_{ij}, \quad (2)$$

where $\hat{A}_{ij}^\dagger = \frac{1}{2}\sum_\sigma \sigma \hat{b}_{i\sigma}^\dagger \hat{b}_{j\bar{\sigma}}^\dagger$ and $\hat{B}_{ij}^\dagger = \frac{1}{2}\sum_\sigma \hat{b}_{i\sigma}^\dagger \hat{b}_{j\sigma}$ are singlet operators, invariant under $SU(2)$ transformations of the spinor $(\hat{b}_{i\uparrow}, \hat{b}_{i\downarrow})$ and :: means normal order. The identities $\hat{B}_{ij}^\dagger \hat{B}_{ij} = 2(\hat{\mathbf{S}}_i + \hat{\mathbf{S}}_j)^2$ and $\hat{A}_{ij}^\dagger \hat{A}_{ij} = 2(\hat{\mathbf{S}}_i - \hat{\mathbf{S}}_j)^2$ reveal the ferromagnetic and antiferromagnetic character of each term of (13), respectively. Hence, the possible coexistence of both kinds of correlations renders this scheme of calculation ideal to investigate frustrated quantum antiferromagnets [25, 26, 28, 29, 30, 31].

The mean field decoupling of (13) is performed in such way that $A_{ij} = \langle \hat{A}_{ij} \rangle = \langle \hat{A}_{ij}^\dagger \rangle$ and $B_{ij} = \langle \hat{B}_{ij} \rangle = \langle \hat{B}_{ij}^\dagger \rangle$. Then, after introducing the local constraint on average through a Lagrange multiplier λ, the diagonalized mean field Hamiltonian becomes

$$\hat{H}_{\mathrm{MF}} = E_{\mathrm{gs}} + \sum_{\mathbf{k}} \omega_{\mathbf{k}} \left[\hat{\alpha}_{\mathbf{k}\uparrow}^\dagger \hat{\alpha}_{\mathbf{k}\uparrow} + \hat{\alpha}_{-\mathbf{k}\downarrow}^\dagger \hat{\alpha}_{-\mathbf{k}\downarrow} \right]. \quad (3)$$

Here

$$E_{\rm gs} = \frac{1}{2}\sum_{\mathbf{k}} \omega_{\mathbf{k}} + \lambda N(S+\frac{1}{2}) \tag{4}$$

is the ground state energy and

$$\omega_{\mathbf{k}\uparrow} = \omega_{\mathbf{k}\downarrow} = \omega_{\mathbf{k}} = [(\gamma^{\rm B}_{\mathbf{k}}+\lambda)^2 - (\gamma^{\rm A}_{\mathbf{k}})^2]^{\frac{1}{2}} \tag{5}$$

is the spinon dispersion relation with geometrical factors $\gamma^{\rm B}_{\mathbf{k}} = \frac{1}{2}J\sum_\delta B_\delta \cos\mathbf{k}.\delta$ and $\gamma^{\rm A}_{\mathbf{k}} = \frac{1}{2}J\sum_\delta A_\delta \sin\mathbf{k}.\delta$, and the sums run over all the vectors δ connecting the first neighbors of the triangular lattice with N sites. The mean field parameters have been chosen real and satisfy the relations $B_\delta = B_{-\delta}$ and $A_\delta = -A_{-\delta}$ [28]. The mean field free energy is given by

$$F = E_{\rm gs} + T\sum_{\mathbf{k}\sigma} \ln\left(1 - e^{-\beta\omega_{\mathbf{k}\sigma}}\right), \tag{6}$$

whose minimization with respect to the mean field parameters, A_δ, B_δ and λ leads to the following self-consistent equations:

$$\begin{aligned} A_\delta &= \frac{1}{2N}\sum_{\mathbf{k}} \frac{\gamma^{\rm A}_{\mathbf{k}}}{\omega_{\mathbf{k}}}\,(1+2\,n_{\mathbf{k}})\sin\mathbf{k}.\delta, \\ B_\delta &= \frac{1}{2N}\sum_{\mathbf{k}} \frac{(\gamma^{\rm B}_{\mathbf{k}}+\lambda)}{\omega_{\mathbf{k}}}\,(1+2\,n_{\mathbf{k}})\cos\mathbf{k}.\delta, \\ S+\frac{1}{2} &= \frac{1}{2N}\sum_{\mathbf{k}} \frac{(\gamma^{\rm B}_{\mathbf{k}}+\lambda)}{\omega_{\mathbf{k}}}\,(1+2\,n_{\mathbf{k}}), \end{aligned} \tag{7}$$

with $n_{\mathbf{k}} = (e^{\beta\omega_{\mathbf{k}}}-1)^{-1}$ the bosonic occupation number. As previously stated, the advantage of the SBMF is to be able to study finite temperature rotationally invariant phase of the triangular AF, dictated by the Mermin-Wagner theorem [20, 21]. In particular, the numerical self consistent solutions of (7) correspond to the renormalized classical regime with an exponential decay of the spin correlation functions characterized by the magnetic wave vector $\mathbf{Q} = (\frac{4\pi}{3}, 0)$ of the 120° Néel structure [32]. This manifests in the gapped spinon dispersion $\omega_{\mathbf{k}}$ with minimum at $\mathbf{k} = \pm\frac{\mathbf{Q}}{2}$. The finite temperature gap prevents the infrared divergences from appearing in the theory. At low temperatures the gap is exponentially small, becoming $\omega_{\pm\frac{\mathbf{Q}}{2}} \sim 1/N$ in the $T \to 0$ limit. Formally, one should first perform $N \to \infty$ and then take the limit $T \to 0$ to recover the $SU(2)$ broken symmetry state. In analogy with the Bose condensation phenomena, this procedure requires one to treat separately the singular modes of (7) and transform the sums into integrals. This gives a new set of equations with the quantum corrected local magnetization m as a new self consistent parameter, while λ is adjusted so as to get a gapless spinon dispersion in each iteration. Then, antiferromagnetism is interpreted as a quantum fluid where the condensate of the up/down bosons at $\pm\frac{\mathbf{Q}}{2}$ and the normal fluid of bosons correspond to the spiraling magnetization m and the zero point quantum fluctuations, respectively [24]. Alternatively, we have worked with large finite systems. This procedure is simpler because the same set (7) are used for the $T \neq 0$ and $T = 0$

cases. Although the mean field solutions keep their rotational invariant character, the local magnetization m can be obtained by relating it to the static structure factor $S(\mathbf{k}) = \sum_{\mathbf{R}} e^{i\mathbf{k}.\mathbf{R}} \langle \mathrm{gs}|\hat{S}_0 . \hat{S}_{\mathbf{R}}|\mathrm{gs}\rangle$ evaluated at $\mathbf{k} = \mathbf{Q}$ and the singular modes as [23]

$$\frac{1}{2N} \frac{(\gamma^{\mathrm{B}}_{\frac{\mathbf{Q}}{2}} + \lambda)^2}{\omega^2_{\frac{\mathbf{Q}}{2}}} = S(\mathbf{Q}) = \frac{N}{2} m^2,$$

where the last line of (7) has been used. For the triangular $S = \frac{1}{2}$ AF the local magnetization of the 120° Néel ground state gives $m = 0.275$ (We have checked that this procedure is equivalent to solve the new set of equations above mentioned with self consistent parameters A_δ, B_δ and m and the sums transformed into integrals). This value should be compared with the quantum Monte Carlo result [7], $m_{\mathrm{QMC}} = 0.205(1)$. The underestimate of the zero point quantum fluctuations can be attributed to both the mean field approximation and the relaxation of the local constraint which violates the physical Hilbert space. In the next section, we will show that the latter leads to some unphysical magnetic excitations in the spectrum, requiring a careful analysis of the low lying energy excitations to properly compute the low temperature properties of the THM.

3. SBMF low lying magnetic excitations

To analyze the magnetic excitations of the THM within the SBMF approximation we compute the $T = 0$ spin-spin dynamic structure factor,

$$S^{zz}(\mathbf{k}, \omega) = \sum_n |\langle \mathrm{gs}|\mathbf{S}^z_{\mathbf{k}}|n\rangle|^2 \delta(\omega - (\epsilon_n - E_{\mathrm{gs}})), \tag{8}$$

where $|n\rangle$ are mean field excited states, and $\mathbf{S}^z_{\mathbf{k}}$ is the Fourier transforms of $\mathbf{S}^z_i$. We have recently shown that (8) takes the simple form [28]

$$S^{zz}(\mathbf{k}, \omega) = \sum_{\mathbf{q}} |u_{\mathbf{k}+\mathbf{q}} v_{\mathbf{q}} - u_{\mathbf{q}} v_{\mathbf{q}+\mathbf{k}}|^2 \delta(\omega - (\omega_{-\mathbf{q}} + \omega_{\mathbf{k}+\mathbf{q}})), \tag{9}$$

where $u_{\mathbf{k}} = [\frac{1}{2}(1 + \frac{\gamma^{\mathrm{B}}_{\mathbf{k}} + \lambda}{\omega_{\mathbf{k}}})]^{\frac{1}{2}}$ and $v_{\mathbf{k}} = \mathrm{i}\,\mathrm{sgn}(\gamma^{\mathrm{A}}_{\mathbf{k}})[\frac{1}{2}(-1 + \frac{\gamma^{\mathrm{B}}_{\mathbf{k}} + \lambda}{\omega_{\mathbf{k}}})]^{\frac{1}{2}}$ are the coefficients of the Bogoliubov transformation that diagonalizes $\hat{H}_{\mathrm{MF}}$. It is clear from (9) that the spin-spin dynamical structure factor consists of two spinon excitations which gives a continuum of spin-1 excitations. Furthermore, since we are working with finite systems whose mean field solution does not break the $SU(2)$ symmetry, $S^{xx} = S^{yy} = S^{zz}$. Nevertheless, as the system size increases, and the 120° Néel correlations are developed, there is a distinction among the two-spinon processes that can be observed in figure 1(a), where an intensity plot of (9) in energy-momentum space is shown. Notice that, in order to show the contribution at all energies, the intensity is plotted in a logarithmic scale. The main signal of $S^{zz}(\mathbf{k}, \omega)$ (intense red curves) corresponds to the microscopic processes of destroying one spinon $b_{\pm\frac{\mathbf{Q}}{2}\sigma}$ of the condensate and creating another one $b^\dagger_{\mathbf{k}\pm\frac{\mathbf{Q}}{2}\sigma}$ in the normal fluid and viceversa; while the blue region corresponds to the creation of

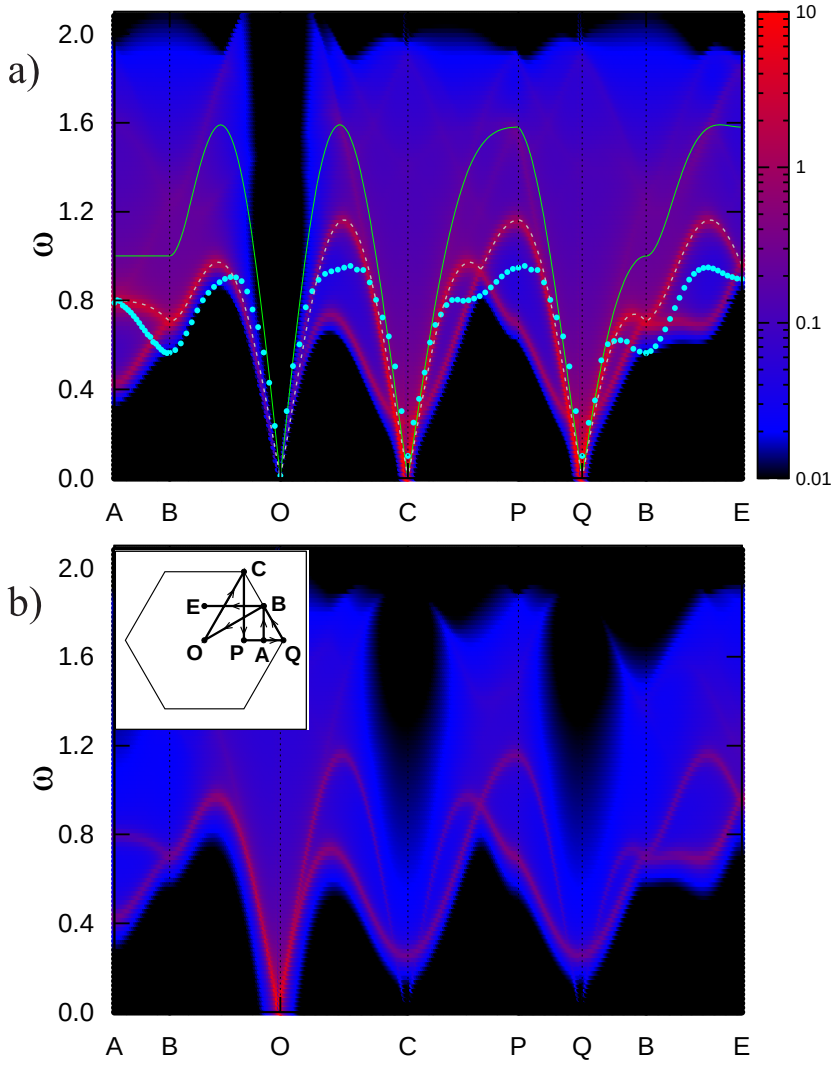

Figure 1. Dynamical structure factors along the path shown in the inset of (b). (a) Magnetic structure factor within the Schwinger boson mean field (9) (Intensity curves); LSWT results (solid green line); series expansion results [10] (blue dots). The reconstructed dispersion relation $\overline{\omega}_{\mathbf{k}}$ is shown in dashed line. (b) Density-density dynamical structure factor (11). The intensity scale is logarithmic as in (a)

two spinons in the normal fluid only [28]. The energy cost of the former two spin-$\frac{1}{2}$ spinon excitation is just $\omega_{\mathbf{k}\mp\frac{\mathbf{Q}}{2}}$, since in the thermodynamic limit $\omega_{\mp\frac{\mathbf{Q}}{2}} \to 0$. Notice that at low energies these shifted spinon based dispersions reproduce quite well the LSWT results (solid green line) which describe the semiclassical long range transverse distortions of the 120° Néel order. On the other hand, at higher energies, where the LSWT semiclassical description is no longer valid, the spectral weight between both shifted spinonic bands is redistributed in such a way that if one reconstructs a new dispersion $\overline{\omega}_{\mathbf{k}}$ from those pieces of spinon dispersions with dominant spectral weight (dashed line), the main features of the series expansion results [10] (blue points) are recovered. There is, however, an additional remnant weak signal which we attribute

to the relaxation of the local constraint of the mean field approximation. To quantify the relative spectral weight between $\overline{\omega}_{\mathbf{k}}$ and the weak band, note that in the best case –at $\mathbf{k}=Q$– the contribution of $\overline{\omega}_{\mathbf{k}}$ represents around 95% of the total weight while the weak band only 2%. On the other hand, in the worst case – middle point of OC – the contributions are 50% and 20%, respectively. To describe the physical Hilbert space of the spin operators the local constraint of Schwinger bosons must be satisfied exactly, $\hat{\mathbf{S}}_i^2 = \frac{n_i}{2}(\frac{n_i}{2}+1)$. So, no fluctuations of the number of boson per site should be allowed. However, as the constraint is taken into account on average there appear unphysical spin fluctuations in $S(\mathbf{k},\omega)$ coming from such density fluctuations which can be investigated through the density-density dynamical structure factor defined as,

$$N(\mathbf{k},\omega) = \sum_n |\langle \mathrm{gs}|\mathrm{n}_{\mathbf{k}}|\mathrm{n}\rangle|^2 \delta(\omega - (\epsilon_\mathrm{n} - \mathrm{E}_{\mathrm{gs}})), \tag{10}$$

where $n_{\mathbf{k}}$ is the Fourier transform of $n_i = \sum_\sigma b_{i\sigma}^\dagger b_{i\sigma}$. After a little of algebra it results in

$$N(\mathbf{k},\omega) = \sum_{\mathbf{q}} |u_{\mathbf{k}+\mathbf{q}} v_{\mathbf{q}} + u_{\mathbf{q}} v_{\mathbf{q}+\mathbf{k}}|^2 \delta(\omega - (\omega_{-\mathbf{q}} + \omega_{\mathbf{k}+\mathbf{q}})). \tag{11}$$

In figure 1(b), (11) is plotted in energy-momentum space. It is observed that the dominant spectral weight of the density-density dynamical structure factor $N(\mathbf{k},\omega)$ coincides with the weak signal of $S^{zz}(\mathbf{k},\omega)$ (figure 1(a)). This notable resemblance led us to identify the remnant signal of $S^{zz}(\mathbf{k},\omega)$ with the unphysical spin fluctuations originating from the density fluctuations of the Schwinger bosons [28]. Therefore, we expect that after projecting the mean field ground state $|\mathrm{gs}\rangle$ into the constrained Hilbert space of $2S$ bosons per site such unphysical excitations will disappear.

So far the reconstructed dispersion corresponds to a spin-1 excitation made of two spin-$\frac{1}{2}$ free spinons. Then, the relevant question is whether the spinons are bound or not once one goes beyond mean field theory. This issue has been addressed for frustrated AF within the context of effective gauge field theories [33, 34]. In particular, for a commensurate spinon condensed phase, it is expected that the fluctuations of the emergent gauge fields confine the spinon excitations, giving rise to the spin-1 magnon of the 120° Néel order. While this kind of calculation is out of the scope of our present work, we can get some indication of the above physical picture by a simple calculation. Let us split the original Hamiltonian as $H = H_{\mathrm{MF}} + V$, with the interaction term given by $V = H - H_{\mathrm{MF}}$. The effect of V on a two free spinon state $|2\mathrm{s}\rangle = |\mathbf{q}\sigma;\mathbf{p}\sigma\rangle = \alpha_{\mathbf{q}\sigma}^\dagger \alpha_{\mathbf{p}\sigma}^\dagger |\mathrm{gs}\rangle$ can be estimated, to first order in perturbation theory, by computing the energy of creating two spinons above the ground state as $E_{2\mathrm{s}} = \langle 2\mathrm{s}|H|2\mathrm{s}\rangle - \langle \mathrm{gs}|H|\mathrm{gs}\rangle$. Then, the interaction between the two spinons is obtained as $v_{\mathrm{int}} = \overline{E}_{2\mathrm{s}} - E_{2\mathrm{s}}^{MF}$ where $E_{2\mathrm{s}}^{MF} = \langle 2\mathrm{s}|H_{MF}|2\mathrm{s}\rangle - \langle \mathrm{gs}|H_{MF}|\mathrm{gs}\rangle = \omega_{\mathbf{q}\sigma} + \omega_{\mathbf{p}\sigma}$ and $E_{2\mathrm{s}}$ is rescaled as $\overline{E}_{2\mathrm{s}} = \frac{2}{3} E_{2\mathrm{s}}$ in order to compensate the difference, $\langle \mathrm{gs}|H|\mathrm{gs}\rangle = \frac{3}{2}\langle \mathrm{gs}|H_{MF}|\mathrm{gs}\rangle$, resulting between our mean field decoupling and the application of Wick's theorem which corresponds to a fully self consistent Hartree-Fock-Bogoliubov decoupling [30] (Note that this $\frac{2}{3}$ has nothing to do with the *ad hoc* factor of Arovas and Auerbach [20, 21]). The interaction thus calculated give

$$v_{\rm int} = \frac{1}{3N}\Big[\gamma_{\mathbf{q}-\mathbf{p}}\Big(u_{\mathbf{q}}^2 u_{\mathbf{p}}^2 + |v_{\mathbf{q}}|^2|v_{\mathbf{p}}|^2 + 2u_{\mathbf{q}}v_{\mathbf{q}}u_{\mathbf{p}}v_{\mathbf{p}}\Big) + \\ + 2\gamma_{\mathbf{q}+\mathbf{p}}\Big(u_{\mathbf{q}}^2|v_{\mathbf{p}}|^2 + u_{\mathbf{p}}^2|v_{\mathbf{q}}|^2 - 2u_{\mathbf{q}}v_{\mathbf{q}}u_{\mathbf{p}}v_{\mathbf{p}}\Big) + 9J\Big], \tag{12}$$

by the present mean field where $\gamma_{\mathbf{k}} = \frac{1}{2}\sum_\delta J_\delta \cos\mathbf{k}\cdot\delta$. For a physical excitation $|2{\rm s}\rangle = |\pm\frac{\mathbf{Q}}{2}\sigma;\mathbf{k}\mp\frac{\mathbf{Q}}{2}\sigma\rangle$, involving the creation of one spinon in the condensate and another one in the normal fluid, it is easy to check numerically the attractive character of (12). In particular, when the total two spinon momentum is $\mathbf{k}=B$ the energy binding is $v_{\rm int}\sim -0.16J$, while the energy cost to create the two free spinons above the ground state is $\omega_{\frac{\mathbf{Q}}{2}\sigma}+\omega_{B-\frac{\mathbf{Q}}{2}\sigma}\sim 0.7J$. On the other hand, when the two spinons are created in the condensate the interaction becomes $|v_{\rm int}|\sim O(Nm^2)$, meaning an infinite attraction for the spinons that build up the magnons at the Goldstone modes $\mathbf{k}=0,\pm\mathbf{Q}$. Even if this instability is an artifact of the first order correction, we believe that this simple calculation lends support to the physical picture of tightly bound spinons in the neighborhood of the Goldstone modes while at higher energies they remain weakly bound. Of course, this statement should be addressed by a more rigorous calculation [35, 36].

4. Low temperature properties

As pointed out in the introduction, the SBMF ground state properties like energy, magnetic wave vector, magnetization and spin stiffness are not significantly affected by the relaxation of the local constraint [25, 28, 30]. However, as soon as temperature increases the system starts to explore in increasingly large amounts an unphysical phase space due to the fluctuations of the density of Schwinger bosons. Consequently, the SBMF becomes inadequate to describe the low temperature properties. In this section we will show that it is possible to modify the SBMF in order to get reliable results for the low temperature regime of the THM. First, we assume that at the temperatures considered, the spinons are sufficiently bound in such way that the relevant physical excitations can be envisaged as spin-1 excitations with the reconstructed dispersion relation $\overline{\omega}_{\mathbf{k}}$ defined above. On the other hand, in order to mimic the projection to the physical phase space -not considered in the mean field- we discard the unphysical excitations. We have renamed this calculational scheme as reconstructed Schwinger boson mean field (RSBMF). We will mainly focus on the importance of the roton-like excitations to explain the high values of entropy found at intermediate temperatures ($T\sim 0.3J$) [6, 10]. Although the RSBMF solutions correspond to the renormalized classical regime, it is worth stressing that we do not expect to fully recover the expected behaviour near the zero temperature transition. In fact, it is well known that the correlation length at the mean field level has an extra exponent in temperature dependence of the preexponential factor when compared with the predictions of effective field theories based on the NLσM or confined spinons near the zero temperature

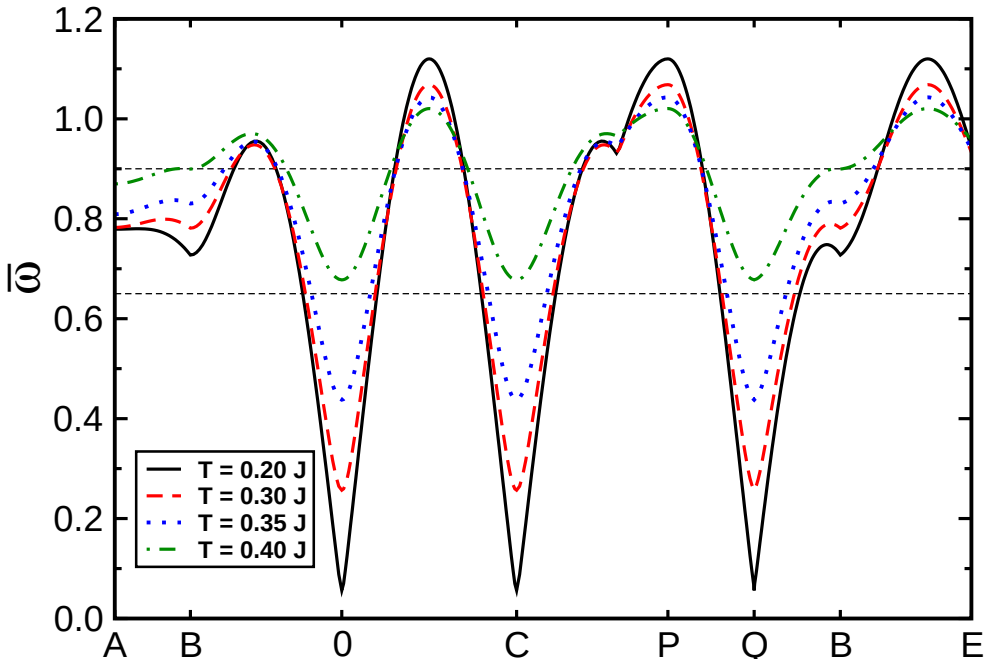

Figure 2. Temperature dependence of the reconstructed dispersion relation, as defined in the text, along the path of the inset of figure 1. The horizontal dashed lines correspond to the energy intervals used in figure 4.

transition [35, 36]. We have found non trivial solutions, $A_\delta, B_\delta \neq 0$, for the self consistent equations (7) up to $T \sim 0.42J$. For $T > 0.42J$ the finite temperature phase of the triangular AF becomes a perfect paramagnet with no intersite correlations. Such a phase has no analog in the interacting spin problem, so it is an artifact of the mean field or large-N approximation. In fact, the effect of finite N corrections to this unwanted transition has been investigated in the literature [37]. In any case, since the available results of HTE are reliable down to $T \sim 0.3J$ we will concentrate on the temperature range $0 - 0.42J$ in order to interpolate between other results.

In figure 2 is shown the temperature dependence of the reconstructed dispersion $\overline{\omega}_{\mathbf{k}}$. As temperature increases, a narrowing of the bandwidth along with the opening of a gap and a flattening of the roton-like excitations is observed. The entropy per site corresponding to these low energy spin-1 excitations is

$$\mathcal{S} = \frac{1}{N} \sum_{\mathbf{k}} [\, (\overline{n}_{\mathbf{k}} + 1) \, \ln (\overline{n}_{\mathbf{k}} + 1) - \overline{n}_{\mathbf{k}} \, \ln \overline{n}_{\mathbf{k}} \,] \,, \tag{13}$$

where the reconstructed dispersion $\overline{\omega}_{\mathbf{k}}$ is plugged in the averaged occupation number $\overline{n}_{\mathbf{k}} = (e^{\beta \overline{\omega}_{\mathbf{k}}} - 1)^{-1}$. In contrast, when the two free spinon species are considered (SBMF) the resulting entropy per site is

$$\mathcal{S} = \frac{1}{N} \sum_{\mathbf{k}\sigma} [\, (n_{\mathbf{k}\sigma} + 1) \, \ln (n_{\mathbf{k}\sigma} + 1) - n_{\mathbf{k}\sigma} \, \ln n_{\mathbf{k}\sigma} \,] \,, \tag{14}$$

where the spinon excitations $\omega_{\mathbf{k}\sigma}$ are plugged in the occupation number $n_{\mathbf{k}\sigma}$ and the sum over the two spinon species is taken into account. In figure 3 it is shown that the

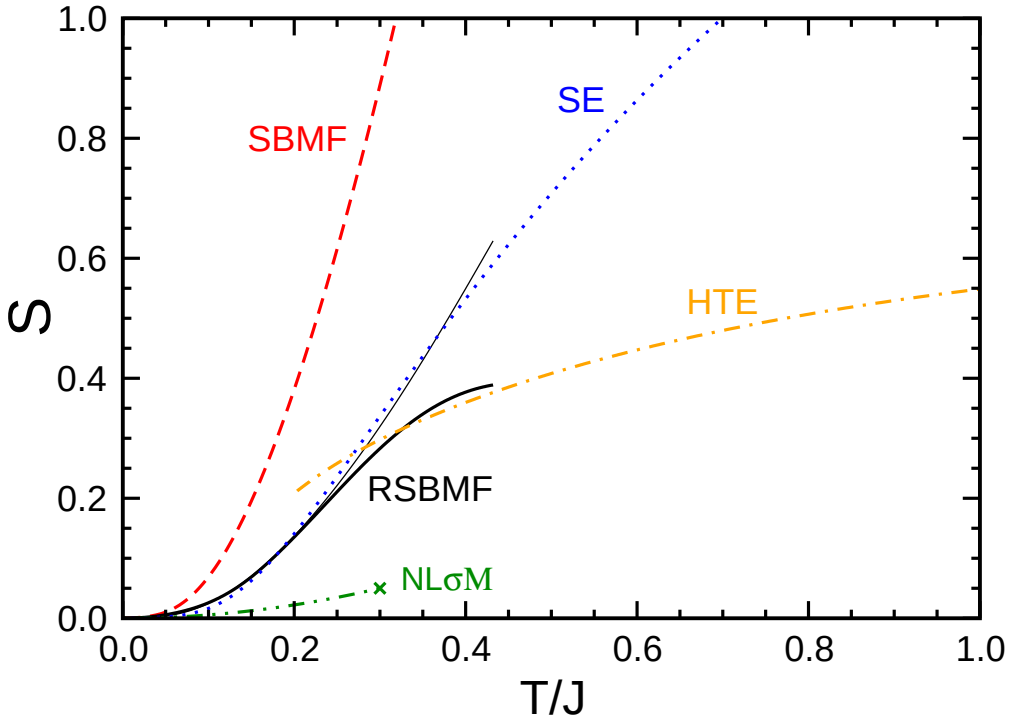

Figure 3. Temperature dependence of the entropy computed within the RSBMF (13) (black solid line); SBMF (14) (red dashed line); HTE [6] (orange dotted-dashed line); SE [10] (blue dotted line) and NLσM [10](green double dotted-dashed line). The black thin solid line represents the SBMF result divided by 2.785 (see text in section 5).

RSBMF entropy (black solid line) interpolates quite well between the expected values at zero temperature and $T \sim 0.3J$ predicted by HTE (orange dotted-dashed line); while the high values of the SBMF entropy (red dashed line) are due to the inclusion of the spurious excitations. To complement these results, also shown in figure 3 is the entropy corresponding to the low energy spin-1 excitations with the dispersion relation found with SE at zero temperature (blue dotted line) and that of the NLσM [10]. The agreement with SE is very good at low temperatures, although the RSBMF entropy is better aligned with HTE at higher temperatures. This difference can be attributed to the fact that the SE entropy has been computed with the $T = 0$ dispersion relation while in the RSBMF entropy the reconstructed dispersion relation is temperature dependent (see figure 2).

To discern between the contribution of the magnonic low energy excitation and the high energy roton-like excitations we have computed the entropy for different ranges of energy [10]. The blue dashed line of figure 4 represents the contribution of the low energy modes while the red dotted-dashed line represents the low energy plus the roton modes. In agreement with [10] it can be observed that the increasing contribution of the roton modes starts from $T \sim 0.1J$. As a reference we have included the entropy value predicted by the NLσM at $T = 0.3J$ (black cross) which agrees reasonably with the low energy contribution of the RSBMF. The apparently counter-intuitive decreasing of the

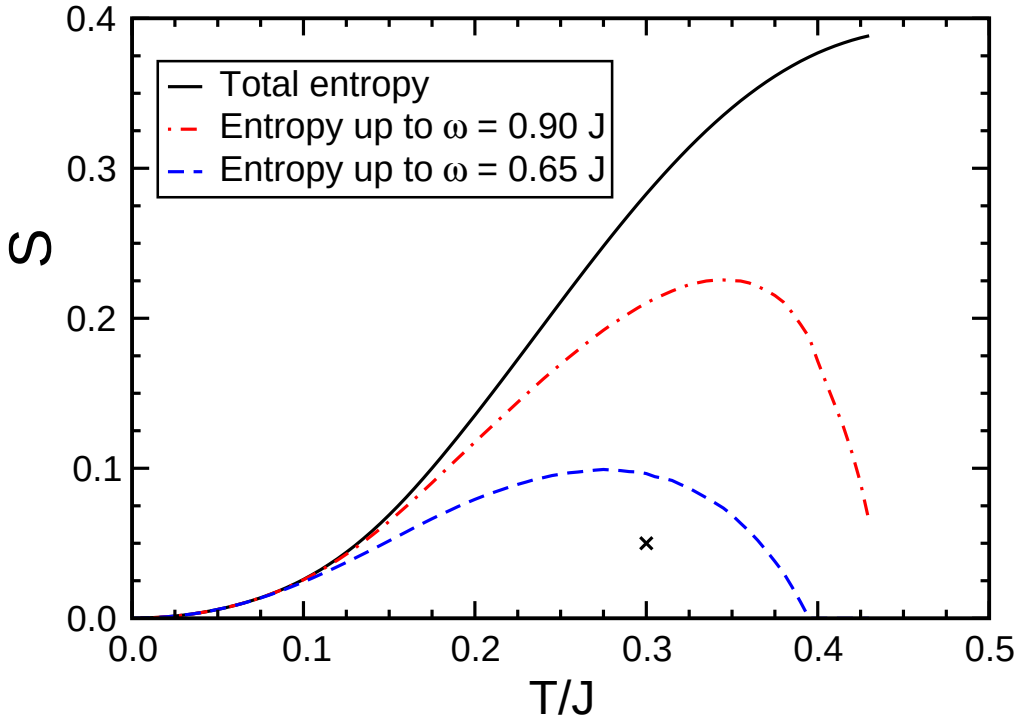

Figure 4. Temperature dependence of the RSBMF entropy computed for different range of energies. The cross indicates the entropy value predicted by the non linear sigma model (NLσM) at $T = 0.3J$.

partial entropies at larger temperatures is due to the temperature dependence of $\overline{\omega}_{\mathbf{k}}$. In the case of a temperature independent dispersion [10] it is expected an increasing contribution for all energy intervals because of the increasing occupation number average for each mode. In our case, instead, the effect of temperature is to push up an important amount of modes outside the corresponding energy intervals, lowering its contribution to the partial entropy for $T \geq 0.3J$. For instance, the minimum of the dispersion at $T = 0.4J$ is greater than $0.65J$, then the contribution of this energy interval to the entropy is zero. Similarly, within the energy interval $0 - 0.9J$, the decreasing of the entropy at $T = 0.4J$ is due to the fact that the rotonic part of the dispersion flattens and crosses the top of the interval $0 - 0.9J$.

Taking into account the above mentioned we conclude that at least within the range $0.1J - 0.3J$ the contribution of the rotonic modes becomes relevant to the total entropy. In particular, these results confirm the idea that the higher values of entropy found with HTE around $T \sim 0.3J$ can be attributed to the contribution of the roton excitations. Recently, we have related the roton-like excitations with AF collinear fluctuations above the 120° Néel order [28]. In fact, it is easy to check that by including frustrating interactions to second neighbors (J_2) the roton excitations soften, becoming the precursor of the transition to a collinear state at $J_2/J \sim 0.16$ [39]. Then, within the context of the RSBMF, the high values of entropy at low temperatures can be related to the contribution of AF collinear fluctuations signalled by the flattening of the dispersion

relation around the midpoint of the edges of the triangular Brillouin zone. This effect is missed in the NLσM, where only the effective low energy modes are taken into account.

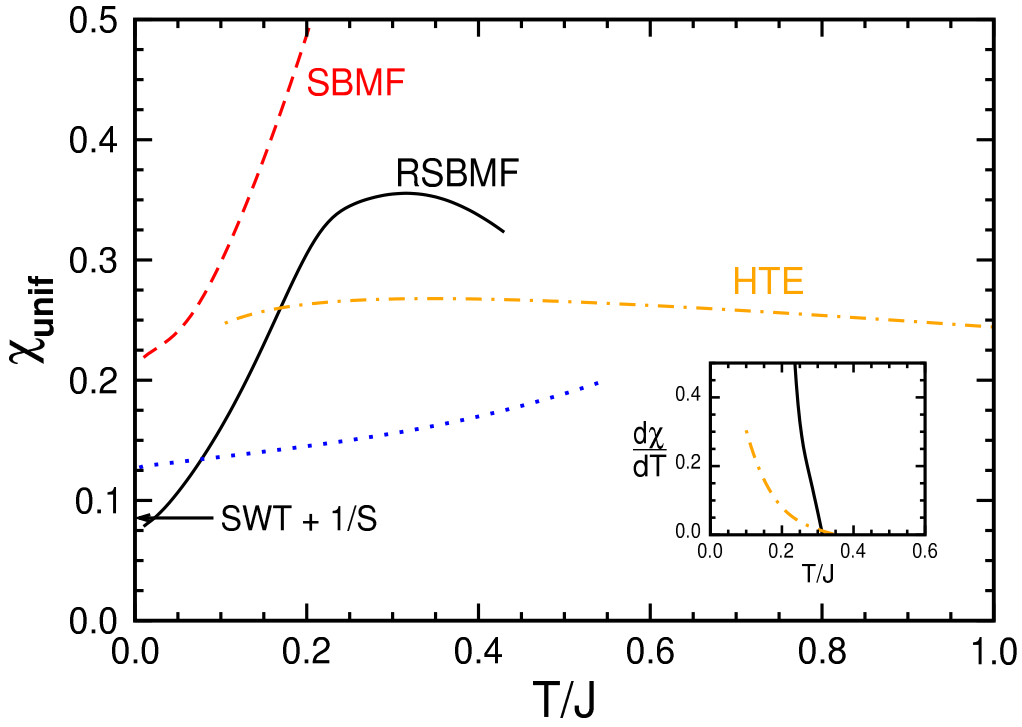

Figure 5. Temperature dependence of the uniform susceptibility. RSBMF (15)(Solid black line); SBMF (16) (red dashed line); HTE of [6] (orange dotted dashed line) and SBMF computed within the one singlet operator scheme as in [32, 40] (blue dotted line). The arrow indicates the averaged $T = 0$ result of the linear spin wave theory plus $1/S$ corrections of [41]. Inset: temperature derivative of the uniform susceptibility versus temperature.

The uniform susceptibility calculated within the RSBMF gives

$$\chi_{\rm u} = \frac{S(0)}{T} = \frac{1}{N}\sum_{\mathbf{k}} \overline{n}_{\mathbf{k}}(\overline{n}_{\mathbf{k}}+1) \tag{15}$$

where $S(0)$ is the finite temperature static structure factor $S(\mathbf{q}) = \sum_{\mathbf{R}} < \hat{\mathbf{S}}_0.\hat{\mathbf{S}}_{\mathbf{R}} > \exp(i\mathbf{q}.\mathbf{R})$ evaluated at $\mathbf{q} = 0$; while in SBMF it results

$$\chi_{\rm u} = \frac{1}{N}\sum_{\mathbf{k}} n_{\mathbf{k}}(n_{\mathbf{k}}+1). \tag{16}$$

In figure 5 is shown the uniform susceptibility calculated within the RSBMF (black solid line) and the SBMF (red dashed line). Consistent with the previous entropy results, the uniform susceptibility is overestimated by the SBMF. That is, the presence of the spurious magnetic excitations enhances the response of the system to a uniform magnetic field. On the other hand, the RSBMF results interpolates quite well between the expected zero temperature value (see arrow) and HTE results of [6] (orange dotted-dashed line). In particular, the extrapolated zero temperature value is $\chi_{\rm u} \sim 0.072$

which should be compared with $\chi_{\rm u} \sim 0.084$, corresponding to the averaged spin wave results plus $1/S$ corrections [15]. At very low temperatures the RSBMF behaves as $\chi_{\rm u} \sim 0.072 + 0.6T$ while the behaviour expected for classical renormalized regime [15] is $\chi_{\rm u} \sim 0.084 + 0.07T$. The one order of magnitude in the slope is related to the fact that the true correlation length increases faster than the mean field solutions as zero temperature is approached (see [15, 36]). For $T > 0.15J$ the uniform susceptibility differs from HTE results in contrast to the excellent agreement obtained for the entropy. While entropy depends on the correct counting of states, through the reconstructed dispersion $\overline{\omega}_{\mathbf{k}}$, the uniform susceptibility is related to the spectral weight distribution at $\mathbf{k} = 0$ which at these temperatures, probably, is not correctly taken into account by the mean field approximation. For instance, we have assumed that the pair of spinons building up the spin-1 excitations at $\mathbf{k} = 0$ are sufficiently bound. Therefore, the required lowering of the uniform susceptibility to recover the HTE results would be consistent with a weaker bound spinon regime for $T > 0.15J$. Another source of the above mentioned discrepancy can be attributed to the omission of the continuum contribution to the uniform susceptibility. Notice, however, that despite the rounded peak of the HTE is broader than the RSBMF they are both located approximately at the same temperature position, $T \sim 0.35J$ [6]. This can be noticed in the inset of figure 5 where the temperature derivative of $\chi_{\rm u}$ versus temperature is plotted. For completeness, we also show the SBMF prediction within the one singlet operator scheme (blue dotted line), previously performed in [32, 40]. In this case the interpolation is not good because this scheme of calculation fails to reproduce the low energy spectrum of the THM [28].

Finally, at low temperatures (below $T \sim 0.1J$), the specific heat behaves quadratically as $C_v \sim a(T/J)^2$, with $a = 7.3$ and $a = 5.2$ for SBMF and RSBMF, respectively. As a reference, the latter value should be compared with $a = 5.3(2)$, resulting from an HTE interpolation method [42], specially developed for the low temperature specific heat behaviour; while $a \sim 3.4$ is found by plugging in the spin wave velocities of the THM in the Debye construction.

5. Discussion

Here we discuss the validity of the RSBMF developed to compute the low temperature properties of the THM. Originally, the THM was investigated within SBMF based on the one singlet operator (A_{ij}) scheme. As this scheme gives a wrong sum rule, $\int \sum_{\mathbf{k}\alpha} S^{\alpha\alpha}(\mathbf{k},\omega) d\omega = \frac{3}{2} NS(S+1)$, it is well known [20, 21] that an *ad hoc* factor of $2/3$ is needed to compensate the overcounting of the number of degrees of freedom. For the present two singlet scheme there is no need of *ad hoc* factors since already at the mean field level (SBMF) the sum rule is fulfilled. Furthermore, it has been shown that Gaussian corrections for the ground state energy and spin stiffness of the THM improve significantly the accuracy of the SBMF results when compared with exact diagonalization results on finite systems [25].

Regarding the magnetic excitations, we have defined a reconstructed dispersion $\overline{\omega}_{\mathbf{k}}$ – guided by the dominant spectral weight of the spin-spin dynamic structure factor– which reproduces quite well the series expansion results. In addition, we found unphysical excitations related to the fluctuations of the density of Schwinger bosons due to the relaxation of the local constraint. Unfortunately, it is difficult to compute the Gaussian corrections for the dynamical structure factor to improve the local constraint. Consequently, to mimic the projection of the SBMF into the physical Hilbert space we have discarded the spurious excitations. This allowed us to define the reconstructed Schwinger boson mean field, based on bosonic spin-1 excitations with the reconstructed dispersion $\overline{\omega}_{\mathbf{k}}$.

Given that the RSBMF thus defined is not rigorously justified we have followed an alternative route to confirm whether the counting of the degree of freedom is correctly taken into account, at least approximately, within the RSBMF. To do that we have concentrated on the entropy for the two-spin problem. In this case the problem can be solved exactly and in the high temperature limit the entropy is $\mathcal{S}_{\rm ex} = 2\ln(2S+1)$. On the other hand, the SBMF prediction can be worked out analytically, giving $\mathcal{S}_{\rm MF} = 2\ln[(S+1)^{2S+2}/S^{2S}]$. For $S = 1/2$, it is found that $\mathcal{S}_{\rm MF} = 2.785\ \mathcal{S}_{\rm ex}$. Therefore, the factor 2.785 gives a faithful compensation of the SBMF entropy due to the wrong counting. Notably, if the SBMF entropy (red dashed line) of figure 3 is divided by the factor 2.785 (see black thin solid line of figure 3) the RSBMF entropy (black solid line) of figure 3 is recovered, at least within the temperature range $0 - 0.3J$ of interest. This agreement gives further support to our RSBMF procedure.

Another possible procedure is to implement the local constraint numerically by using a valence bond basis but sign problems, already at the variational level, appear in the Quantum Monte Carlo calculation [43]. More recently, a permanent algorithm was used to compute ground state energies on the kagomé lattice within the context of projected Schwinger bosons. Although the method seems to circumvent the sign problem, only systems up to $N = 36$ size has been studied [44].

6. Concluding remarks

We have investigated the low temperature properties of the triangular-lattice Heisenberg model with a bosonic spinon theory based on the Schwinger boson mean field theory. Using the two singlet operator scheme of calculation and by analyzing the spin-spin and density-density dynamical structure factors we can distinguish between the physical magnetic excitations, which reproduce the series expansion results, and the spurious excitations that result from the relaxation of the local constraint on the number of bosons per site. By assuming that *i*) the effect of projecting into the physical Hilbert space can be mimiced by getting rid of the latter excitations and *ii*) that an attractive residual interaction binds the spinons, we obtain a reconstructed Schwinger boson mean field with low energy spin-1 excitations with the reconstructed 'physical' dispersion relation. A comparison with reliable $T = 0$ and high temperature ($T \gtrsim 0.3J$) results

reveal that the RSBMF thus defined provides a very good interpolation for many thermodynamic properties like entropy, uniform susceptibility and specific heat over the temperature range $0 \leq T \lesssim 0.3J$, which is difficult to access by other methods. One of our main physical results is to confirm the idea [10] that the high values of entropy found with HTE are due to the excitation of roton excitations which, within the context of our theory, can be identified with the collinear short range AF fluctuations above the underlying 120° Néel correlations [28]. An alternative interpretation has been proposed in [45], using the physics of the XXZ Heisenberg model as a starting point. Here a low energy effective theory is constructed in terms of fermionized vortices where vortex-antivortex excitations on the honeycomb (dual) lattice are related to the roton excitations. Interestingly, the dependence of the roton excitations with spatial anisotropy resembles that with temperature found in the present work. Even if the description in terms of fermionized vortices recovers the roton excitations predicted by SE [10, 16], the present bosonic approach seems to be more appropriate to describe all the expected features of the isotropic AF Heisenberg model, that is, the 120° Néel order, the correct Goldstone mode structure and the roton excitations. In any case it would be interesting to investigate the validity range of each approach by performing a close comparison between them.

The simplicity of the RSBMF along with the consistent description of several features of the THM like static ground state properties, energy spectrum and low temperature thermodynamic properties give strong support to the bosonic spinon hypothesis to interpret the physics of the triangular-lattice Heisenberg model. Of course, the present approximation should be refined by using many body diagrammatic techniques [35] or by performing 1/N corrections [30]. Work in this direction is in progress.

Finally, we believe that a proper extension of the present theory to the anisotropic XXZ case would allow one to investigate the unusual magnetic features of the recently found [46, 47, 48] inorganic spin-1/2 triangular antiferromagnets, $Ba_3CoSb_2O_9$ and $Ba_3CuSb_2O_9$. An experimental realization of the related XY model has been proposed recently in the area of ultra-cold atoms in optical lattice potentials [49, 50].

Acknowledgments

This work is supported in part by CONICET (PIP 1948), ANPCyT (PICT R1776) and by the US National Science Foundation grant number DMR-1004231.

References

[1] Anderson P W 1973 *Mater. Res. Bull.* **8** 153
[2] Fazekas P and Anderson P W 1974 *Phil. Mag.* **30** 423
[3] Huse D A and Elser V 1988 *Phys. Rev. Lett.* **60** 2531
[4] Bernu B, Lhuillier C and Pierre L 1992 *Phys. Rev. Lett.* **69** 2590
[5] Leung P W and Runge K J 1993 *Phys. Rev. Lett.* **47** 5861

[6] Elstner N, Singh R R P and Young A P 1993 *Phys. Rev. Lett.* **71** 1629
[7] Capriotti L, Trumper A E and Sorella S 1999 *Phys. Rev. Lett.* **82** 3899
[8] Kruger S E, Darradi R, Richter J and Farnell D J J 2006 *Phys. Rev.* B **73** 094404
[9] White S R and Chernyshev A L 2007 *Phys. Rev. Lett.* **99** 127004
[10] Zheng W, Fjaerestad J O, Singh R R P, McKenzie R H and Coldea R 2006 *Phys. Rev.* B **74** 224420
[11] Mezzacapo F and Cirac J I 2010 *New J. Phys.* **12** 103039
[12] Jolicoeur Th and Le Guillou J C 1989 *Phys. Rev.* B **40** 2727
[13] Azaria P, Delamotte B and Mouhanna D 1992 *Phys. Rev. Lett.* **68** 1762
[14] Chubukov A V, Senthil T and Sachdev S 1994 *Phys. Rev. Lett.* **72** 2089
[15] Chubukov A V, Sachdev S and Senthil T 1994 *Nucl. Phys.* B **426** 601
[16] Zheng W, Fjaerestad J O, Singh R R P, McKenzie R H and Coldea R 2006 *Phys. Rev. Lett.* **96** 057201
[17] Starykh O A, Chubukov A V and Abanov A G 2006 *Phys. Rev.* B **74** 180403
[18] Chernyshev A L and Zhitomirsky M E 2006 *Phys. Rev. Lett.* **97** 207202
[19] Chernyshev A L and Zhitomirsky M E 2009 *Phys. Rev.* B **79** 144416
[20] Arovas D P and Auerbach A 1988 *Phys. Rev.* B **38** 316
[21] Auerbach A and Arovas D P 1988 *Phys. Rev. Lett.* **61** 617
[22] Mermin N D and Wagner H 1966 *Phys. Rev. Lett.* **17** 1133
[23] Hirsch J E and Tang S 1989 *Phys. Rev.* B **39** 2850
[24] Chandra P, Coleman P and Larkin A I 1990 *J. Phys.: Condens. Matter* **2** 7933
[25] Manuel L O, Trumper A E and Ceccatto H A 1998 *Phys. Rev.* B **57** 8348
[26] Gazza C J and Ceccatto H A 1993 *J. Phys.: Condens. Matter* **5** L135
[27] Lecheminant P, Bernu B, Lhuillier C and Pierre L 1995 *Phys. Rev.* B **52** 9162
[28] Mezio A, Sposetti C N, Manuel L O and Trumper A E 2011 *Europhys. Lett.* **94** 47001
[29] Ceccatto H A, Gazza C J and Trumper A E 1993 *Phys. Rev.* B **47** 12329
[30] Trumper A E, Manuel L O, Gazza C J and Ceccatto H A 1997 *Phys. Rev. Lett.* **78** 2216
[31] Flint R and Coleman P 2009 *Phys. Rev.* B **79** 014424
[32] Yoshioka D and Miyazaki J 1991 *J. Phys. Soc. Japan* **60** 614
[33] Read N and Sachdev S 1991 *Phys. Rev. Lett.* **66** 1773
[34] Sachdev S and Read N 1991, Int. J. Mod. Phys. B **5** 219
[35] Chubukov A 1991 *Phys. Rev.* B **44** 12318
[36] Chubukov A V and Starykh O A 1995 *Phys. Rev.* B **52** 440
[37] Tchernyshyov O and Sondhi S L 2002 *Nucl. Phys.* B **639** 429
[38] Mila F 1990 *Phys. Rev.* B **42** 2677
[39] Manuel L O and Ceccatto H A 1999 *Phys. Rev.* B **60** 9489
[40] Sachdev S 1992 *Phys. Rev.* B **45** 12377
[41] Chubukov A V, Sachdev S and Senthil T 1994 *J. Phys.: Condens. Matter* **6** 8891
[42] Bernu B and Misguich G 2001 *Phys. Rev.* B **63** 134409
[43] Sindzingre P, Lecheminant P and Lhuillier C 1994 *Phys. Rev.* B **50** 3108
[44] Tay T and Motrunich O I 2011 *Phys. Rev.* B **84** 020404
[45] Alicea J, Motrunich O I and Fisher M P A 2006 *Phys. Rev.* B **73** 174430
[46] Shirata Y, Tanaka H, Matsuo A and Kindo K 2012 *Phys. Rev. Lett.* **108** 057205
[47] Wiebe C R 2012 private communication
[48] Zhou H D, Choi E S, Li G, Balicas L, Wiebe C R, Qiu Y, Copley J R D and Gardner J S 2011 *Phys. Rev. Lett.* **106** 147204
[49] Schmied R, Roscilde T, Murg V, Porras D and Cirac J I 2008 *New J. Phys.* **10** 045017
[50] Hauke P, Roscilde T, Murg V, Cirac J I and Schmied R 2010 *New J. Phys.* **12** 053036